

*Supplement of*

**Using different assumptions of aerosol mixing state and chemical composition to predict CCN concentrations based on field measurement in Beijing**

**Jingye Ren<sup>1</sup>, Fang Zhang<sup>1\*</sup>, Yuying Wang<sup>1</sup>, Xinxin Fan<sup>1</sup>, Xiaoai Jin<sup>1</sup>, Weiqi Xu<sup>2,3</sup>, Yele Sun<sup>2,3</sup>, Maureen Cribb<sup>4</sup>, Zhanqing Li<sup>1,4</sup>**

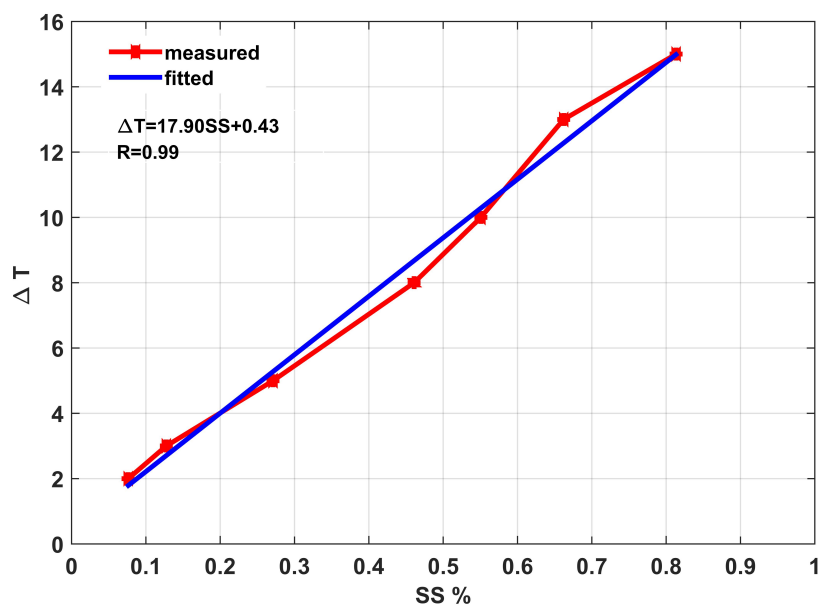
*<sup>1</sup>State Key Laboratory of Earth Surface Processes and Resource Ecology, College of Global Change and Earth System Science, Beijing Normal University, Beijing 100875, China*

*<sup>2</sup>State Key Laboratory of Atmospheric Boundary Layer Physics and Atmospheric Chemistry, Institute of Atmospheric Physics, Chinese Academy of Sciences, Beijing 100029, China*

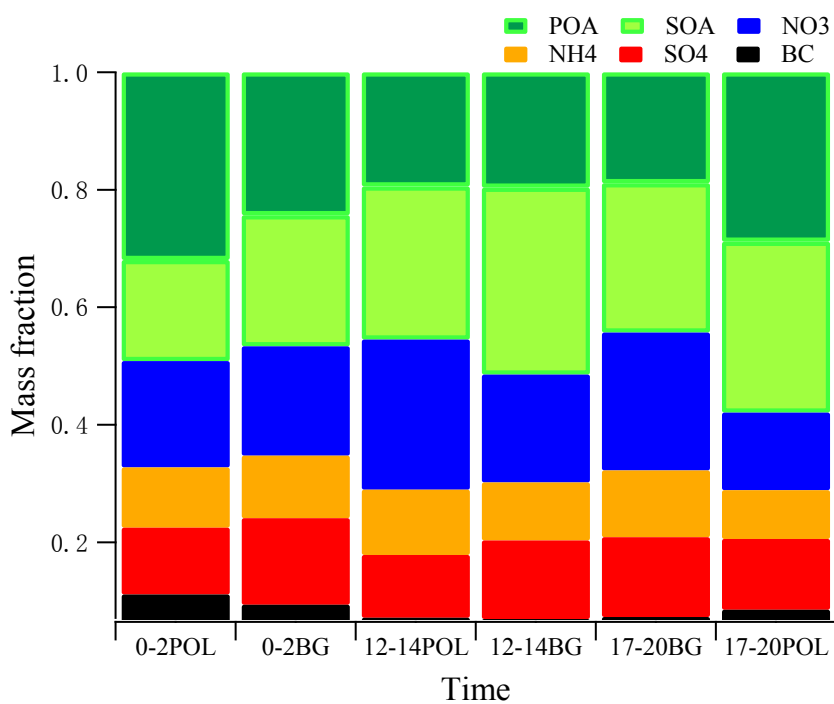
*<sup>3</sup>University of Chinese Academy of Sciences, Beijing 100049, China*

*<sup>4</sup>Earth System Science Interdisciplinary Center and Department of Atmospheric and Oceanic Science, University of Maryland, College Park, Maryland, USA*

**\*Correspondence to: Fang Zhang (fang.zhang@bnu.edu.cn)**

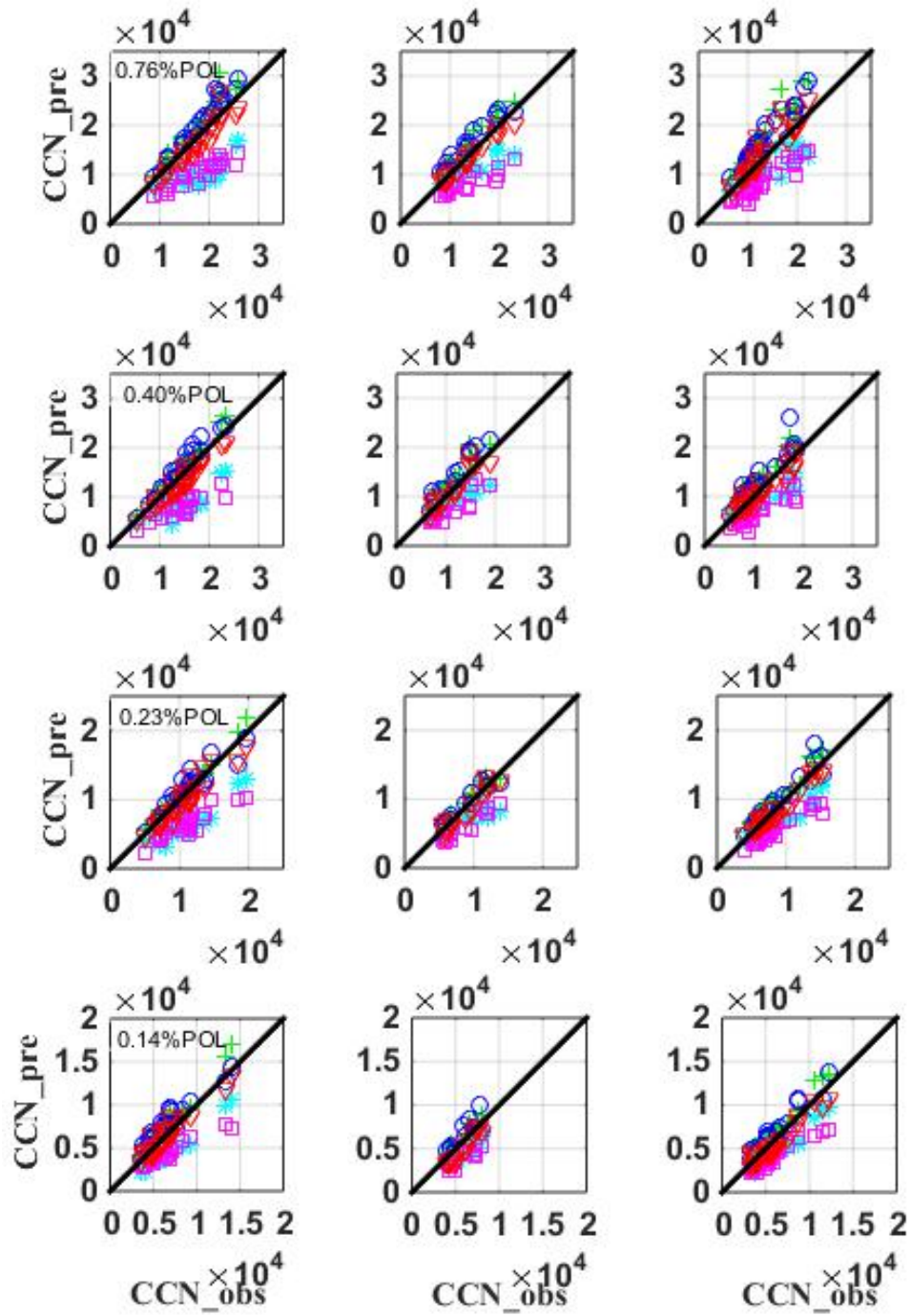


**Figure S1.** Temperature gradient curve for different supersaturations, the ammonium sulfate is used to calibrate the supersaturations levels of the CCNc, with the longitudinal temperature gradients of 2, 3, 5, 8, 10, 13, 15 K.



**Figure S2.** The variations of bulk chemical composition mass concentration fraction during three selected periods (0000–0200 LT, 1200–1400 LT, 1700–2000 LT) under

background and polluted conditions.



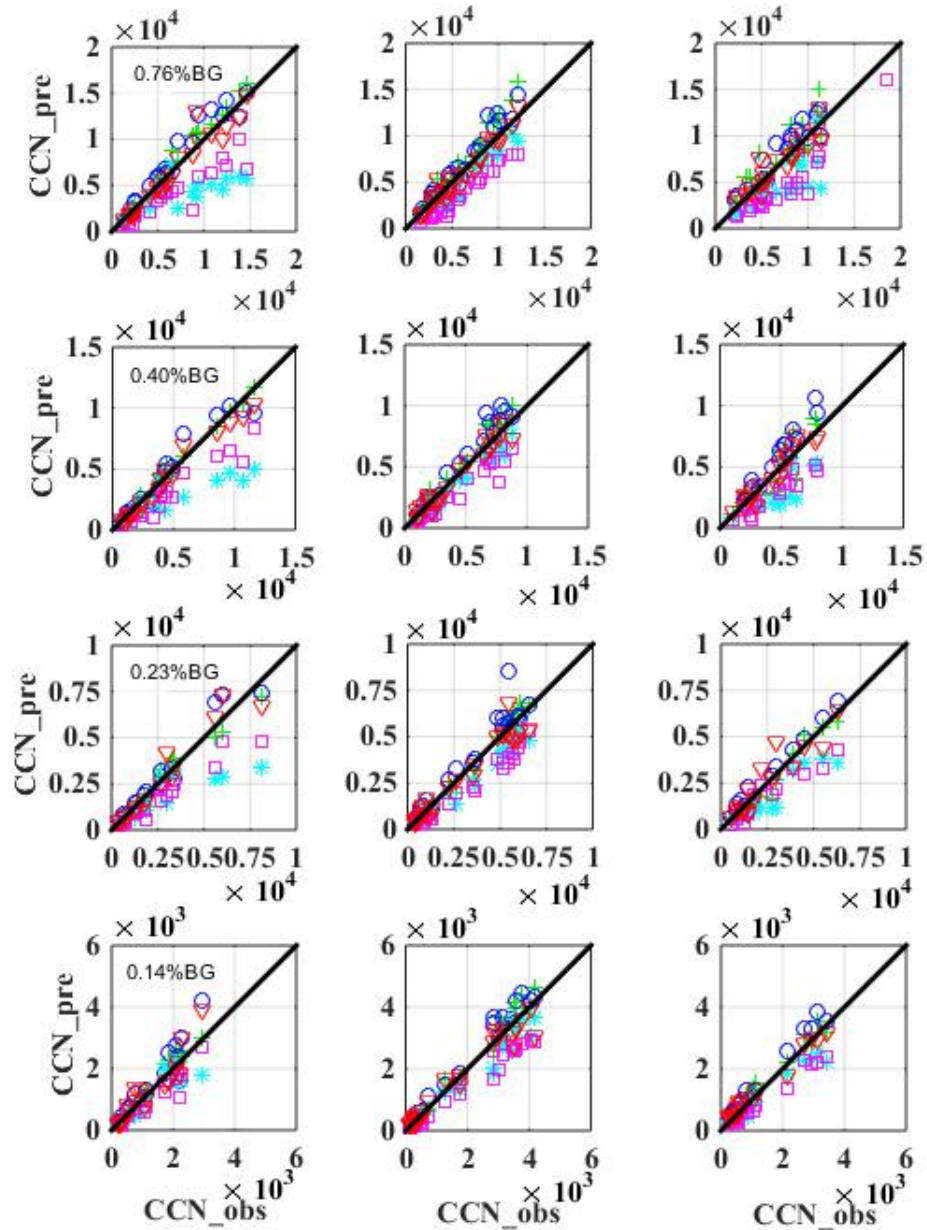


**Figure S3.** The comparisons of predicted  $N_{CCN}$  with measured  $N_{CCN}$  using five assumptions at four supersaturations, 0.14, 0.23, 0.40, 0.76%, during four emission periods under background and polluted conditions. Each plot from left to right is 0000–0200 LT, 1200–1400 LT and 1700–2000 LT, respectively.

**Table S1.** Summary of the critical diameter during three selected periods (0000–0200 LT, 1200–1400 LT, 1700–2000 LT) under polluted and background conditions.

| SS%  | 0-2POL      | 0-2BG        | 12-14POL    | 12-14BG      | 17-20POL    | 17-20BG      |
|------|-------------|--------------|-------------|--------------|-------------|--------------|
| 0.12 | 178.07±7.72 | 188.30±20.88 | 169.10±6.32 | 174.47±12.72 | 174.06±9.32 | 185.42±18.40 |
| 0.14 | 138.41±7.79 | 139.54±18.23 | 132.01±6.72 | 137.58±12.88 | 137.74±9.31 | 146.55±15.10 |
| 0.23 | 90.94±6.06  | 88.00±6.76   | 92.43±6.93  | 92.25±10.34  | 99.24±7.83  | 96.90±10.54  |
| 0.40 | 63.32±6.91  | 62.08±5.33   | 72.47±6.22  | 67.86±9.10   | 77.63±8.57  | 71.45±11.69  |
| 0.76 | 45.97±7.22  | 44.82±5.71   | 51.95±4.78  | 47.24±6.10   | 57.61±5.75  | 51.25±7.95   |

**Table S2.** Summary of the maximum active fraction during three selected periods (0000–0200 LT, 1200–1400 LT, 1700–2000 LT) under polluted and background conditions.

| SS%  | 0-2POL    | 0-2BG     | 12-14POL  | 12-14BG   | 17-20POL  | 17-20BG   |
|------|-----------|-----------|-----------|-----------|-----------|-----------|
| 0.12 | 0.83±0.03 | 0.83±0.05 | 0.88±0.01 | 0.87±0.06 | 0.87±0.02 | 0.78±0.08 |
| 0.14 | 0.85±0.03 | 0.81±0.04 | 0.90±0.02 | 0.82±0.06 | 0.88±0.03 | 0.80±0.06 |
| 0.23 | 0.89±0.01 | 0.83±0.04 | 0.89±0.02 | 0.84±0.06 | 0.89±0.02 | 0.80±0.05 |
| 0.40 | 0.89±0.01 | 0.85±0.03 | 0.91±0.01 | 0.87±0.04 | 0.90±0.01 | 0.85±0.04 |
| 0.76 | 0.91±0.01 | 0.88±0.02 | 0.92±0.01 | 0.88±0.04 | 0.91±0.01 | 0.88±0.02 |